UNIVERSITY OF LEEDS

This is a repository copy of *Dechlorination of waste polyvinyl chloride (PVC) through non-thermal plasma*.

White Rose Research Online URL for this paper:
https://eprints.whiterose.ac.uk/201929/

Version: Accepted Version

Article:
Song, J., Wang, J. orcid.org/0000-0002-0459-5692, Sima, J. et al. (4 more authors) (Cover date: October 2023) Dechlorination of waste polyvinyl chloride (PVC) through non-thermal plasma. Chemosphere, 338. 139535. ISSN 0045-6535

https://doi.org/10.1016/j.chemosphere.2023.139535

© 2023 Published by Elsevier Ltd. This manuscript version is made available under the CC-BY-NC-ND 4.0 license http://creativecommons.org/licenses/by-nc-nd/4.0/

Reuse
This article is distributed under the terms of the Creative Commons Attribution-NonCommercial-NoDerivs (CC BY-NC-ND) licence. This licence only allows you to download this work and share it with others as long as you credit the authors, but you can't change the article in any way or use it commercially. More information and the full terms of the licence here: https://creativecommons.org/licenses/

Takedown
If you consider content in White Rose Research Online to be in breach of UK law, please notify us by emailing eprints@whiterose.ac.uk including the URL of the record and the reason for the withdrawal request.

White Rose university consortium
Universities of Leeds, Sheffield & York

eprints@whiterose.ac.uk
https://eprints.whiterose.ac.uk/

Dechlorination of waste polyvinyl chloride (PVC) through non-thermal plasma

Jiaxing Song [a], Jun Wang [a], Jingyuan Sima [a], Youqi Zhu [a], Xudong Du [a], Paul T. Williams [b], and Qunxing Huang [a,*]

[a] *State Key Laboratory of Clean Energy Utilization, Institute for Thermal Power Engineering, Zhejiang University, Hangzhou 310027, China*

[b] *School of Chemical and Process Engineering, University of Leeds, Leeds, LS2 9JT, UK*

***Corresponding author**, E-mail: hqx@zju.edu.cn*

Abbreviations	
PVC	Polyvinyl chloride
DBD	Dielectric barrier discharge
NTP	Non-thermal plasma
GC/MS	Gas chromatography/mass spectrometer
Residue-5min	PVC residue treated for 5min
Residue-10min	PVC residue treated for 10min
Residue-20min	PVC residue treated for 20min
Residue-40min	PVC residue treated for 40min

Abstract: Dechlorination is essential for the chemical recycling of waste polyvinyl chloride (PVC) plastics. This study investigated the use of non-thermal plasma (NTP) for chlorine removal, with a focus on the effects of treatment time and discharge power on dechlorination efficiency. The results showed that longer treatment times and higher discharge powers led to better dechlorination

performance. The maximum efficiency (98.25%) and HCl recovery yield (55.72%) were achieved at 180 W power after 40 minutes of treatment where 96.44% of Cl existed in the form of HCl gas, 1.44% in the liquid product, and 2.12% in the solid residue product. NTP at a discharge power of 150 W showed better dechlorination performance compared to traditional thermal pyrolysis treatment in temperatures ranging from 200 to 400 °C. The activation energy analysis of the chlorine removal showed that compared to pyrolysis-based dechlorination (137.09 kJ/mol), NTP-based dechlorination (23.62 kJ/mol) was more easily achievable. This work presents a practical method for the dechlorination of waste PVC plastic using a novel technology without requiring additional thermal and pressure input.

Keywords: Polyvinyl chloride, Plastic wastes, Dechlorination, Non-thermal plasma, Hydrochloric acid

1. Introduction

Polyvinyl chloride (PVC) is the third largest plastic used worldwide, with applications in industries such as electronics, construction, agriculture, and many others [1-4]. In 2021, global PVC production reached 50.70 Mt, resulting in significant amounts of PVC in the waste stream [5]. Thermal recycling methods, such as pyrolysis and gasification, have limited effectiveness when dealing with waste plastics containing PVC, because the chlorine in PVC may contaminate the resulting products [6, 7]. The presence of Cl element will reduce the value of these products, cause equipment corrosion, and result in irreversible environmental pollution. Burning PVC will also produce toxic chlorinated byproducts, including dioxins and polychlorinated biphenyls [8, 9]. Additionally, PVC plastic is

inevitably contained in the mixed waste plastics due to the limitations of the waste sorting process. Therefore, the dechlorination of PVC is essential for sustainable waste plastic recycling in terms of economic and environmental benefits.

Hydrothermal and catalytic pyrolysis have been studied widely as the main disposal methods for dechlorinating waste plastics. Hydrothermal dechlorination tends to operate at high pressures (0.1-19 MPa) and moderate temperatures (220–300 °C) [10-12]. However, it is energy-intensive, requiring harsh reaction conditions, long reaction times, and expensive equipment. Catalytic pyrolysis usually operates at temperatures between 300 and 600 °C in an inert atmosphere and can also remove Cl [13-15]. However, there are problems including high temperatures, equipment corrosion, catalyst deactivation, and high disposal costs [16, 17]. Hence, it is crucial to develop a low-temperature and atmospheric-pressure method for dechlorinating waste plastics.

Non-thermal plasma (NTP), or non-equilibrium plasma, is the fourth state of matter, where the average temperature of gas molecules (10-10^3 °C) is much lower than that of electrons (10^4-10^5 °C). NTP produces high-energy electrons that favor electron collision processes with gases, which could heat the sample to over 200 °C [18, 19]. Additionally, collisions between electrons and gas molecules could create charged particles (cations and anions), and electronically neutral excited substances (radicals, atoms, molecules, and dissociated fragments). These active species have high concentrations and potential energies, leading to many chemical reactions [20-23]. The energy of active species in the N_2 discharge (nitrogen ion, excited atom, and molecules, etc.) was mainly between 6 eV and 11 eV, greater than the energy acquired to break C-C (6.29 eV), C-Cl (4.11 eV), and C-H (3.49 eV) [24]. Therefore, NTP offers a potential method for dechlorinating PVC without requiring additional thermal or pressure input. Currently, the environmental application of NTP was focused on ozone production

[25, 26], air pollution control [27, 28], tar removal [29, 30], and value-added utilization of waste [21, 31]. There is a lack of research on its application for dechlorination.

To achieve dechlorination, this study investigated the use of NTP for the treatment of waste PVC. Specifically, this study investigated the dechlorination efficiency and HCl recovery yield at different treatment times by NTP. This study also explored the effect of NTP discharge power on dechlorination effectiveness and HCl recovery. Additionally, this study compared the dechlorination performance and HCl yield from the NTP at a discharge power of 150 W to thermal pyrolysis treatment at pyrolysis temperatures of 200-400 °C. Finally, a dechlorination mechanism by NTP was proposed. This work provides a novel low-temperature and atmospheric-pressure PVC dechlorination technology, that recovers the HCl by-product simultaneously. It represents a green and promising method for PVC waste treatment.

2. Materials and methods

2.1 Materials and analytical techniques

The PVC plastic polymer used in these experiments was supplied by Shanghai Macklin Biochemical Co., Ltd, China, in the form of powder. It is composed of three elements: C, H, and Cl. The content of C and H was determined through elemental analysis, and the content of Cl was obtained by the difference method. Its elemental composition was analyzed with an elemental analyzer (Vario EL cube), revealing that it contained 38.40 wt.% carbon, 4.80 wt.% hydrogen, and 58.40 wt.% chlorine.

A spectrometer (AvaSpec-ULS2048L-USB2) was applied to record the optical emission spectrum of the NTP, which is a major tool to diagnose the state of gases during discharge. Prior to the experiment, the optical fiber was placed vertically 5 mm away from the discharge gap, and the optical

emission spectrum was measured to investigate the active species in the nitrogen discharge process, with an integration time of 1 s, and an average of 10 measurements.

The released chlorine during the experiments was trapped in deionized water using a bubbler trap, and the concentration of chloride ions was measured using ion chromatography (Dionex Aquion). During analysis, a 125 μL sample was injected into an analytical separation column (Dionex, Ion Pac, AS11-HC) coupled with a guard column (AG11-HC), and the data was collected and processed using Chromaleon software.

To investigate the dechlorination mechanism of PVC, Fourier transform infrared (FTIR) analysis was used to study changes in the functional groups of the polymer during the dechlorination process. The functional groups of the PVC sample and the PVC residue treated after different times were analyzed using an FTIR spectrometer (Nicolet iS50) in the range of 4000–400 cm^{-1} with a resolution of 4 cm^{-1}, and each sample was scanned 32 times.

2.2 Experimental setup

The experimental reactor system is illustrated in Fig. 1. A 0.50 g PVC sample was suspended by quartz wool in the discharge gap between the inner electrode and the ceramic alundum (Al_2O_3) tube, with the outer electrode in close contact with the outer side of the alundum tube. The NTP was generated inside the alundum tube (φ 25×2.50 mm), which was wrapped by a 150 mm-long copper mesh outer electrode. An inner stainless steel electrode rod, 14 mm in diameter, was located at the center of the alundum tube. The stainless steel electrode was connected to an AC high-voltage generator, while the low-voltage electrode was grounded. As a result, the discharge zone was 150 mm in length, and the discharge gap was 3 mm wide. A four-channel digital oscilloscope (MDO3014,

Tektronix, America) monitored the electrical signals. The NTP was generated once the high-voltage generator reached the required power. To assess the dechlorination efficiency, PVC dechlorination experiments were also performed using thermal pyrolysis for comparison. The electric furnace functioned as a heating source during the thermal pyrolysis experiments, and each pyrolysis test was run at constant temperatures ranging from 200 to 400 °C. Before each experiment, nitrogen was purged into the reactor, and it was used as a carrier gas at a flow rate of 100 mL/min. The produced gases passed through a bubbler trap containing 200 mL of deionized water to recover the produced HCl gas. After each experiment, the reactor and the connecting tube between the reactor and the bubbler trap were rinsed with an additional 100 mL of deionized water. The deionized water used for rinsing was mixed with the deionized water in the bubbler trap, ensuring the collection of the majority of HCl. Other gas products, mainly H_2 and N_2, were collected in a gas sample bag. The solid residues were weighed after each experiment to determine the solid yields and were collected for elemental and FTIR analyses.

The yield and compositions of the gas products were determined by gas chromatographs (Agilent 490 Micro GC) equipped with TCD detectors. The gas compositions were analyzed using the 10 m MS5A column held at 80 °C, and argon served as the carrier gas.

The liquid products yield was calculated on mass balance, and composition species were determined using a gas chromatography/mass spectrometer (GC/MS-QP2010 SE, Shimadzu, Japan) equipped with a Shimadzu capillary column (SHRxi-5Sil MS, 30 m × 0.25 mm × 0.25 μm). The GC oven temperature was originally set at 35 °C for 5 min, heated to 300 °C at 15 °C/min, and finally kept constant for 20 min. The mass spectrometer was configured as previously reported [32].

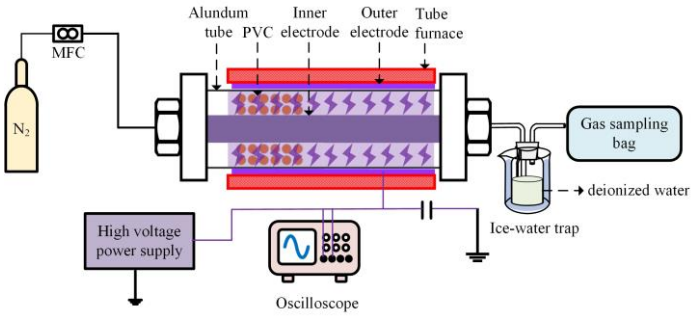

Figure 1 Schematic diagram of the experimental device.

2.3 Dechlorination and element recovery efficiency

The dechlorination efficiency was determined using the following calculation as shown in Eq. (1):

$$Dechlorination\ efficiency = \frac{M_{Cl\ in\ PVC} - M_{Cl\ in\ residue}}{M_{Cl\ in\ PVC}} * 100\% \quad (1)$$

The $M_{Cl\ in\ residue}$ was calculated as Eq. (2):

$$M_{Cl\ in\ residue} = Cl_{utimate\ analysis\ in\ residue} * M_{residue} * 100\% \quad (2)$$

The element recovery efficiency was calculated by Eq. (3) as follows:

$$Element\ recovery\ efficiency = \frac{M_{element\ in\ residue}}{M_{element\ in\ PVC}} * 100\% \quad (3)$$

3. Results and discussion

3.1 Dechlorination under different treatment times

The spectrum of the NTP at the 10th minute of discharge under a power of 180 W is shown in Fig. 2 to identify the active species in the N_2 plasma. The dominant active species bands are the first negative bands of N_2^+ and the second positive bands of N_2 [33]. The spectrum showed emission from N_2^+ at 392 nm, which is a characteristic of N_2 negative glows [34, 35]. The energy level of N_2^+ is high at 18.70 eV. The N_2 second positive band, with an energy level of 11 eV, is the strongest and clearest band of the N_2 spectrum [24, 36]. The energy of both N_2^+ and the second positive band of N_2 are high enough to break the bonds of C-C (6.29 eV), C-Cl (4.11 eV), and C-H (3.49 eV), leading to the

decomposition of PVC.

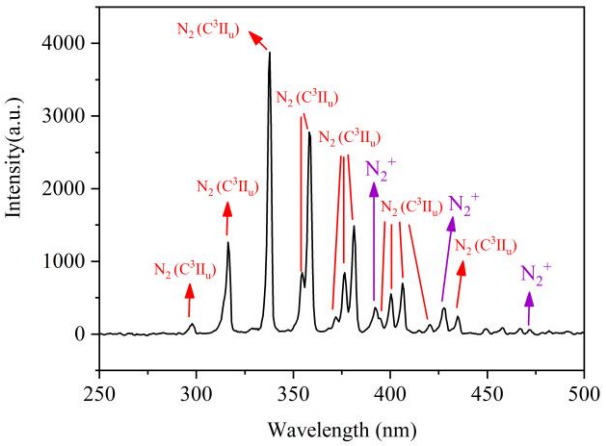

Figure 2 Optical emission spectrum of the NTP in a run.

Fig.3 shows the product distribution, the dechlorination efficiency, and yields of HCl and H_2 under various NTP treatment times at discharge power of 180 W. As shown in Fig. 3(a), with the increase in the NTP treatment time, more PVC sample was decomposed into gas products. The highest gas yield of 56.34% was obtained at a treatment time of 40 min when the yield of liquid products was as low as 5.91%. The liquid products came from the decomposition of the PVC polymer and the secondary reaction of intermediate products.

According to Fig. 3(b), the gas products were primarily composed of HCl and H_2. The bonds of C-Cl and C-H of the PVC sample were broken under the active species of N_2^+ and the second positive band of N_2. Afterwards, part of the radicals of H and Cl combined to form HCl, while part of the H radicals recombined with each other to produce H_2. The HCl yield climbed to 55.72% while the H_2 yield increased to 0.62% when the treatment time was extended to 40 min. It is predicted that lengthening the treatment time would increase both the HCl and H_2 yields, especially the H_2 yield. Increasing the treatment time also increased the dechlorination efficiency, reaching a maximum of 98.25% after NTP treatment of 40 min. It is worth noting that after only 20 min of treatment, the dechlorination efficiency was remarkable, reaching 97.28%.

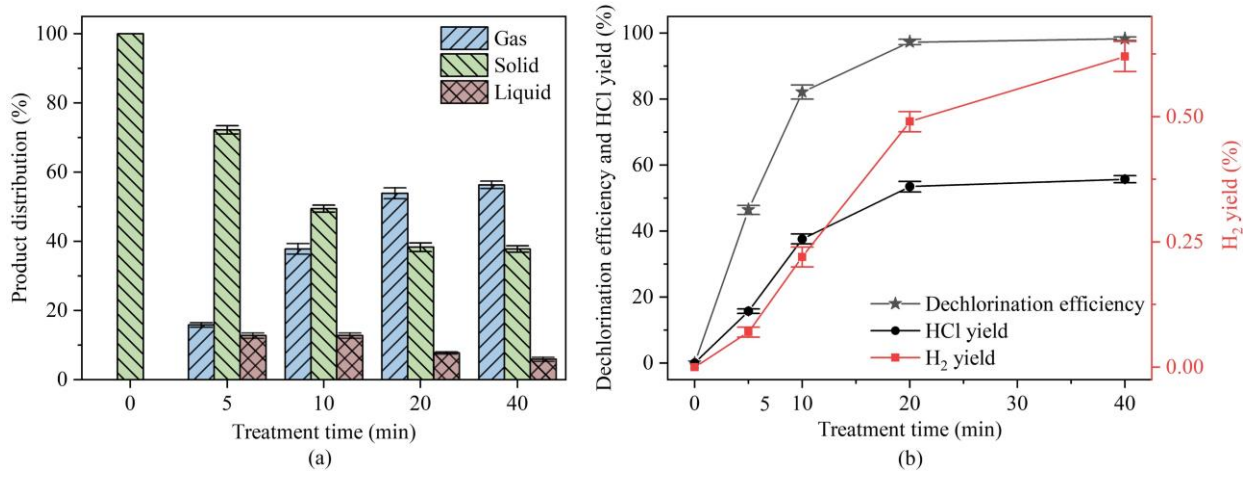

Figure 3 The product distribution (a), and the dechlorination efficiency and yields of HCl and H_2 (b) under various treatment times.

Calculating accurate enthalpy values for dechlorination reactions under NTP is challenging due to their complexity. However, it is well-established that these reactions are exothermic. During the discharge process, electrons acquire energy from the electric field and transfer it to the kinetic and internal energy of the intermediate products through collisions. These energized molecules become excited or ironized, leading to the formation of reactive molecules. Through subsequent collisions, a series of complex physicochemical reactions occur, resulting in the production of final products and the release of heat [37-39]. The reactor temperature during the dechlorination process was measured using a thermocouple. The measurement results are shown in Fig. S1. Fig. S1 indicates that the reactor temperature increased with the treatment time, while the rate of the temperature rise decreased with the treatment time. When the discharge reached 20 min, the reactor temperature was 256.70 °C. At this point, the dechlorination efficiency was 97.28% (Fig. 3(b)), resulting in the weight loss of the PVC sample of 61.70% (Fig. 3(a)). According to the thermal weight loss curve of PVC (Fig. S2), the weight loss of PVC was only 4.67% at this temperature, indicating that the reaction temperature had a minimal impact on the dechlorination effect under NTP. After 40 min of treatment, the final temperature of the

reactor was 279.70 °C.

Fig. 4 and Table S1 display the FTIR spectra and functional groups of various samples, including fresh PVC, PVC residue treated for 5 min under NTP conditions (residue-5min), PVC residue treated for 10 min (residue-10 min), PVC residue treated for 20 min (residue-20min), and PVC residue treated for 40 min (residue-40 min), respectively, with an input power of 180 W. The FTIR was used to observe the development of the reaction throughout different NTP treatment times. After the first 5 min of NTP treatment, the original PVC absorption peaks remained, but new C=C bonds were detected at FTIR wavenumbers at 3015, 811, and 747 cm^{-1}, suggesting dechlorination and dehydrogenation reactions have occurred. Further prolonging the treatment time to 10 min, the C-H bending in -CH2- (2968 cm^{-1}), the C-H bending in -CHCl- (1331, 1255, and 1097 cm^{-1}), and the C-Cl stretching vibration (608 cm^{-1}) disappeared [15, 40]. The results suggested that the H and Cl attached to these functional groups were largely removed after 10 min of treatment using NTP. Meanwhile, new bonds associated with the C=C stretching of aliphatic compositions at 3060, 1599, and 876 cm^{-1} wavenumbers and C=C bonds of aromatic compounds at 1490 cm^{-1} were generated [41]. The aromatic compounds indicated the cyclization of the carbon skeleton during the reaction. The functional groups of residue remained unchanged when the NTP treatment time was increased from 10 to 40 min.

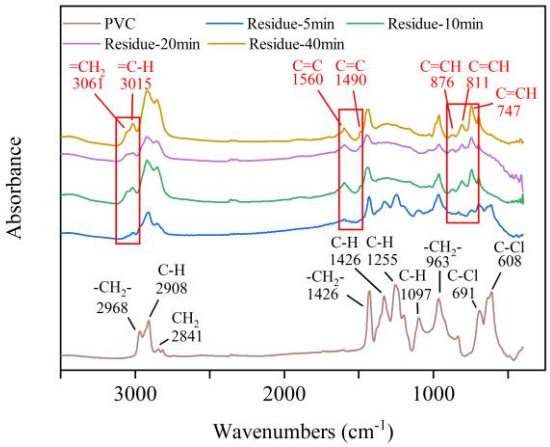

Figure 4 The FTIR spectra of PVC under different treatment times.

Fig. S3(a) displays the distribution of Cl in the products, while Fig. S3(b) shows the recovery efficiency of elements under different treatment times. The Cl distribution in the solid residue decreased as the NTP treatment time was prolonged, as shown in Fig. S3(a). The organic Cl in PVC polymer was mostly converted to inorganic chlorine in the form of HCl gas under the influence of NTP, with the highest Cl distribution of 96.44% towards HCl. After 20 min of treatment, the proportion of Cl in the solid residue dropped to 2.24%, indicating that most of the Cl had been removed. And residual Cl in the solid residue was confirmed by FTIR analysis to exist in the form of -C-Cl- functional groups.

Fig. S3(b) suggests that the C recovery efficiency decreased slightly with the increase in NTP treatment time due to the scission of the carbon skeleton, resulting in the production of liquid by-products. The H recovery efficiency also decreased with increasing treatment time, primarily due to the release of HCl and H_2. In general, element recovery efficiency and dechlorination efficiency showed opposite trends with the prolongation of treatment time. Therefore, it is crucial to find an appropriate dechlorination time.

Table S2 shows the ultimate analysis of the solid residue under different NTP treatment times. When the treatment time increased to 40 min, the Cl content in the solid residue decreased to 3.35 wt.%, and the C content increased to 90.22 wt.%. Moreover, the total content of C and H elements reached 96.26 wt.% after treatment for 40 min. However, the content of elements did not change significantly when the treatment time was further extended from 20 to 40 min, indicating that the solid products reached a relatively stable state after 20 min of treatment. Considering the dechlorination efficiency, HCl yield, and element recovery efficiency, a treatment time of 20 min was considered optimal in this study.

3.2 Dechlorination under different discharge power

The influence of discharge power on the dechlorination effectiveness was investigated at a treatment time of 20 min. Fig. 5 shows the product distribution (Fig. 5(a)), the dechlorination efficiency, and yields of HCl and H_2 (Fig.5(b)) obtained at various discharge powers of NTP. It could be seen in Fig. 5(a) that increasing the NTP discharge power led to a higher gas yield and a lower solid yield. This effect can be attributed to the release of Cl from the siccsion of the C-Cl bonds and the migration of Cl towards the gas phase in the form of HCl. Moreover, the decrease in liquid yield with increasing NTP discharge power from 120 to 180 W indicated that fewer by-products were produced under these conditions.

As displayed in Fig. 5(b), the yields of HCl and H_2 increased with increasing the discharge power, with maximum values of 53.45% and 0.49%, respectively. A minimal dechlorination reaction was observed under a discharge power of 60 W. However, increasing the power to 90 W resulted in a dechlorination efficiency of 46.70%, suggesting the existence of a power threshold between 60 W and 90 W that triggered the dechlorination reaction. The relatively lower dechlorination efficiency observed at 90 W can be attributed to the short treatment time. The dechlorination efficiency increased slightly with increasing the discharge power from 120 to 180 W because the energy was sufficient to remove most of the Cl at the discharge power of 120 W. The majority of Cl removal occurred at a discharge power of 120 W, and the dechlorination efficiency reached 97.05%.

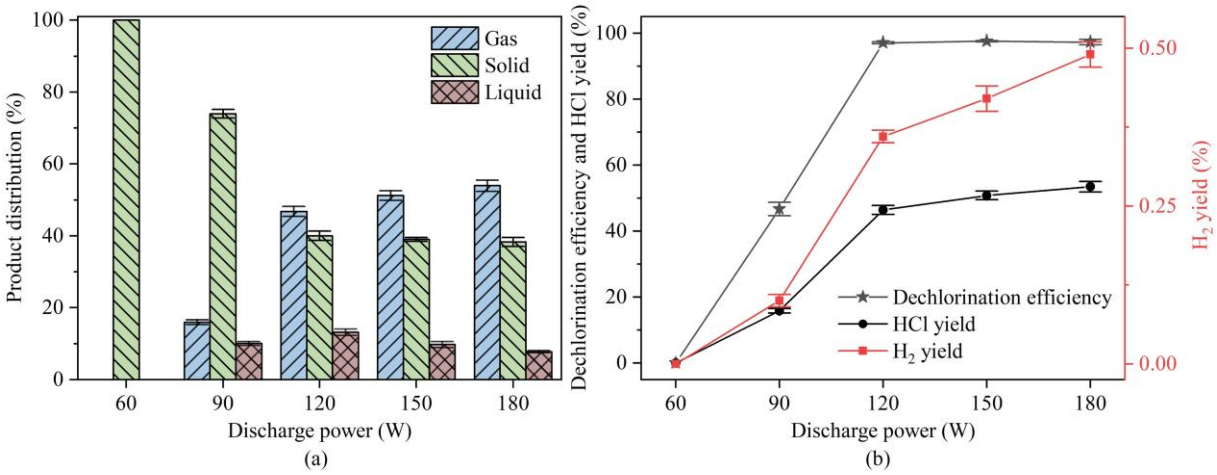

Figure 5 The product distribution (a), and the dechlorination efficiency and yields of HCl and H_2 (b) under various discharge power.

Fig. S4 shows the Cl distribution (Fig. S4(a)) and element recovery efficiency (Fig. S4(b)) obtained at different NTP discharge powers. The results in Fig. S4(a) show that the Cl distribution as HCl increased with increasing discharge power, reaching 91.43% at 180 W. Meanwhile, the Cl content distributed in the solid residue decreased, suggesting a greater dechlorination efficiency.

As shown in Fig. S4(b), the C recovery efficiency gradually decreased to 87.61% when the discharge power was increased to 180 W. Also, the H recovery efficiency declined at higher discharge power. The energy for breaking the C-H bond (3.49 eV) is lower than that for breaking the C-C bond (6.29 eV), so more H radicals are released to form other products, leading to a lower H recovery efficiency.

Table S3 shows the ultimate analysis of the solid residue under various NTP discharge power inputs. With the increase in discharge power, the Cl concentration in the solid residue reduced while the C content in the residue increased. A low Cl concentration and high C content were obtained at a low discharge power of 120 W. The highest overall contents of C and H elements were 96.39 wt.% with a discharge NTP power of 180 W.

3.3 Dechlorination comparison between thermal pyrolysis and NTP

Thermal pyrolysis was applied on PVC dechlorination tests so that the effectiveness of dechlorination could be compared with NTP. When the treatment time was 20 min, the product distribution obtained from thermal pyrolysis experiments conducted between 200 and 400 °C and NTP experiments at an input power of 150 W was illustrated in Fig. 6(a). Fig. 6(b) shows a comparison between thermal pyrolysis results (200 to 400 °C) and NTP results (150 W power) with a treatment time of 20 min in terms of dechlorination efficiency and yields of HCl and H_2. As shown in Fig. 6(a), PVC could not be decomposed until the thermal pyrolysis temperature reached 300 °C, with a solid yield of 93.01%, indicating incomplete pyrolysis. At 400 °C, the solid yield fell to 39.48% while the gas yield was 50.15%. The thermal pyrolysis of PVC takes place in two stages. The first stage, approximately between 200 to 400 °C, involves the removal of most of the Cl, accompanied by the release of small amounts of hydrocarbons [42-44]; The second stage, roughly between 400 to 550 °C, involves the decomposition of dechlorinated PVC to produce other gas and oil products [45-47]. Compared to previous studies, the main decomposition process in this study occurred at a higher temperature of about 400 °C [13, 15, 48]. In contrast, the product distribution from NTP experiments at the discharge power of 150 W was similar to that of thermal pyrolysis at the temperature of 400 °C.

As shown in Fig. 6(b), the yields of HCl by thermal pyrolysis at the temperature of 400 °C and by NTP treatment at the discharge power of 150 W were almost the same. However, the H_2 yield under NTP treatment at 150 W (0.42%) was significantly higher than that under thermal pyrolysis at 400 °C (0.01%). The dechlorination performance using NTP at 150 W was slightly higher than that using thermal pyrolysis at 400 °C by 0.54%. In conclusion, NTP had a better performance on HCl recovery and dechlorination than thermal pyrolysis at a temperature ranging from 200 to 400 °C. 5 g of PVC

was also treated at a discharge power of 150 W for 20 min to assess the dechlorination effectiveness of NTP treatment of PVC on a larger scale. The results showed a dechlorination efficiency of 76.60%, which was lower than the observed efficiency of 97.49% when dechlorinating 0.5 g of PVC. These findings suggest that, in intermittent experiments under the same working conditions, the dechlorination efficiency decreased with an increase in the quantity of the sample being treated.

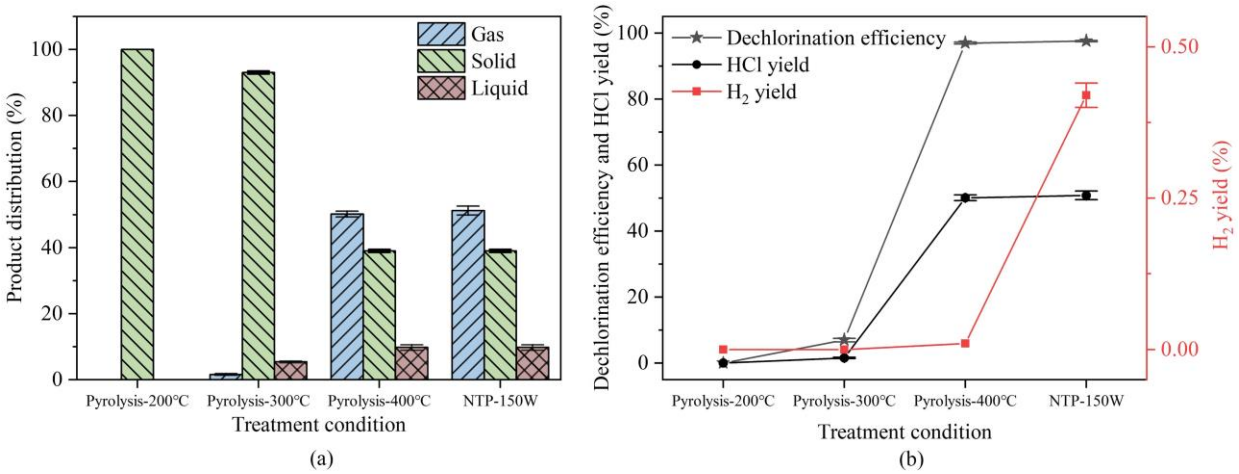

Figure 6 The product distribution(a), and the dechlorination efficiency and yields of HCl and H_2(b) under various treatment conditions.

Fig. S5 shows the Cl distribution (Fig. S5(a)) and element recovery efficiency (Fig. S5(b)) in relation to the thermal pyrolysis temperature (200–400 °C) compared with the NTP results produced at the discharge power of 150 W. It can be seen from Fig. S5(a) that the Cl distribution in the solid residue achieved by the NTP at 150 W was less than that achieved by thermal pyrolysis at 400 °C while the Cl distribution in HCl obtained by the NTP at 150 W was more than that obtained by thermal pyrolysis at 400 °C. The results were consistent with the higher HCl yield and the dechlorination efficiency by the NTP treatment.

As presented in Fig. S5(b), the recovery efficiency of C and H elements under the discharge power of 150 W was lower than that obtained under the thermal pyrolysis temperature of 400 °C, especially

296 the H recovery efficiency. The lower H recovery efficiency obtained by NTP was attributed to a higher
297 transfer of H from the PVC sample to the gas phase.

298 Table S4 shows the ultimate analysis of the solid residue after thermal pyrolysis compared with the
299 NTP process. Compared with the solid residue obtained by thermal pyrolysis at a temperature of
300 400 °C, there was less Cl content and more C content in the solid residue obtained by the NTP at 150
301 W power. However, the NTP process was able to fix a small amount of N element from N_2 into the
302 solid products.

303 The kinetic analysis of the dechlorination using thermal pyrolysis and NTP was discussed. For
304 thermal pyrolysis, the focus was on the temperature range of 200-400 °C, where the dechlorination
305 reaction predominantly takes place. The kinetics of NTP-based dechlorination were calculated using a
306 discharge power of 180 W and a treatment time of 40 min.

307 For a single reaction model, the dechlorination rate at a certain moment can be described by:

308 $$\frac{d\alpha}{dt} = A \exp\left(-\frac{E}{RT}\right)(1-\alpha) \quad (4)$$

309 Where A is the frequency factor; E denotes the activation energy (kJ mol^{-1}); R and T represent the
310 universal gas constant (8.314 J mol^{-1} K^{-1}) and the temperature (K), respectively. α is the conversion
311 which can be expressed by:

312 $$\alpha = \frac{m_0 - m_t}{m_0 - m_f} \quad (5)$$

313 Where m_0, m_t, and m_f are the initial PVC mass, the actual PVC mass and the final residue mass,
314 respectively.

315 With $\beta = \frac{dT}{dt}$, Eq. (1) can be converted into the following form:

316 $$\frac{d\alpha}{dT} = \frac{A}{\beta} exp\left(-\frac{E}{RT}\right)(1-\alpha) \quad (6)$$

317 After the Doyle integral derivation and the Hancock empirical formula, the following equation is

finally obtained:

$$\ln[-ln(1-\alpha)] = -\frac{E}{RT} + ln\left[\frac{AE}{R\beta} - 5.33\right] \quad (7)$$

Where $\ln[-ln(1-\alpha)]$ and $\frac{1}{T}$ exhibit a linear relationship, therefore these two can be fitted into a straight line. The kinetic parameters E and A during different reactions are determined from the slope of $\ln[-ln(1-\alpha)]$ vs. $\frac{1}{T}$ and the intercept of the fitted plot with respect to $\ln[-ln(1-\alpha)]$.

Table S5 shows the comparison of the kinetic parameters using thermal pyrolysis and the NTP approach. The current parameters during thermal pyrolysis progress were similar to those obtained by previous studies [49-51], indicating that the results in this study are reliable. The activation energy required for dechlorinating PVC through thermal pyrolysis was 137.09 kJ/mol, which was approximately 10 times higher than the activation energy (23.62 kJ/mol) for dechlorination through NTP. Therefore, compared to pyrolysis-based dechlorination, NTP-based dechlorination was more easily achievable.

3.4 Reaction mechanism of the dechlorination process by NTP

Fig. 7 illustrates a possible dechlorination mechanism of PVC under NTP conditions. During the process, active substances such as electrons, N_2^+, and the second positive band of N_2 decomposed the PVC polymer into a range of intermediate products including chain hydrocarbons and chlorinated hydrocarbons fragments, as well as radicals. Hydrogen radicals may recombine with each other to form hydrogen, or they can react with Cl radicals to produce HCl, leading to the formation of gas products. Alkenes and alkanes intermediates may undergo hydrogenation and dehydrogenation reactions to convert to each other, while aromatization reactions can generate aromatics. Additionally, the chlorination of alkenes and aromatics may produce chlorinated hydrocarbons and aromatics. Hence, liquid products include four types of compounds: aromatics, chlorinated aromatics, alkanes, and

chlorinated hydrocarbons. The GC/MS analysis of the liquid products is presented in Table S6. Finally, the solid residue left after the dechlorination reaction primarily contained -CH_2-, C=C, and a small amount of -CHCl-.

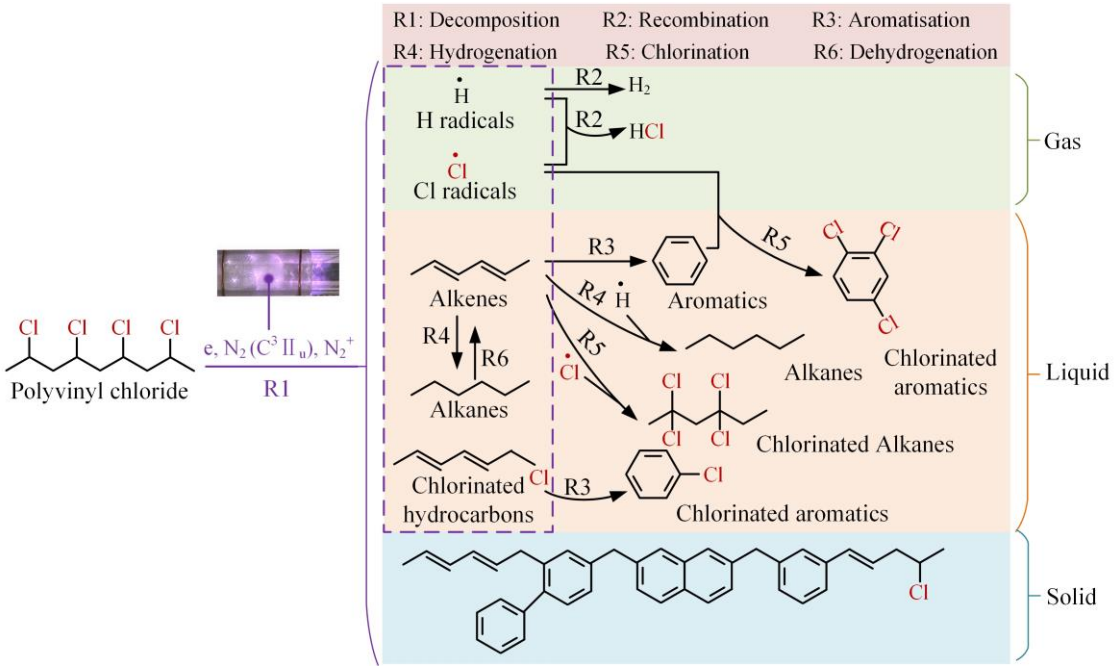

Figure 7 The possible dechlorination mechanism of PVC under NTP.

4. Conclusions

This study investigated the dechlorination efficiency and HCl recovery yield of PVC using NTP at different treatment times and discharge powers. The dechlorination performance and kinetic parameters of dechlorinating PVC were compared with thermal pyrolysis treatment. A possible dechlorination mechanism for PVC using NTP was also presented. The main conclusions were summarized as follows:

(1) The active species in PVC decomposition and subsequent secondary reactions in N_2 plasma mainly consisted of electrons, N_2^+, and the second positive band of N_2.

(2) When treatment time was 40 min, the dechlorination efficiency and HCl recovery yield were up to the maximum value of 98.25% and 55.72%, respectively. However, considering the element

recovery efficiency, a treatment time of 20 min was considered optimal in this study.

(3) After surpassing the threshold power which is between 60 and 90 W, increasing NTP discharge power resulted in higher dechlorination efficiency and HCl recovery yield. However, the dechlorination efficiency decreased with the increase in sample mass under the same working conditions.

(4) The dechlorination reaction was more favorable under NTP treatment (activation energy of 23.62 kJ/mol) than under thermal pyrolysis (activation energy of 137.09 kJ/mol). Additionally, NTP at a discharge power of 150 W exhibited superior performance in dechlorination and HCl recovery than thermal pyrolysis at temperatures ranging from 200 to 400 °C.

Authorship contribution

Jiaxing Song: Writing - original draft, Investigation, Methodology, Writing - review & editing.

Jun Wang: Investigation, Data curation.

Jingyuan Sima: Methodology, Data curation.

Youqi Zhu: Investigation.

Xudong Du: Investigation.

Paul T. William: Investigation.

Qunxing Huang: Supervision, Project administration.

Corresponding Authors

*** Qunxing Huang** - State Key Laboratory of Clean Energy Utilization, Institute for Thermal Power Engineering of Zhejiang University, Hangzhou 310027, China; Phone: +86-571-87952834; Email:

hqx@zju.edu.cn

Note

The author declares no competing financial interest.

Declaration of competing interest

The authors declare that they have no known competing financial interests or personal relationships that could have appeared to influence the work reported in this paper.

Acknowledgments

The authors would like to gratefully acknowledge the National Natural Science Foundation of China (52076190), Key Research and Development Program of Zhejiang province (2023C03129), Zhejiang University Ecological Civilization Plan and the China Scholarship Council.

References

[1]Maisel F, Chancerel P, Dimitrova G, et al. Preparing WEEE plastics for recycling – How optimal particle sizes in pre-processing can improve the separation efficiency of high quality plastics. Resources, Conservation and Recycling. 2020, 154:1-10. https://doi.org/10.1016/j.resconrec.2019.104619.

[2]Pazienza P, De Lucia C. For a new plastics economy in agriculture: Policy reflections on the EU strategy from a local perspective. Journal of Cleaner Production. 2020, 253:1-12. https://doi.org/10.1016/j.jclepro.2019.119844.

[3]Jiang H, Huo R, Zhang Z, et al. Dechlorination performance in chemical looping conversion of polyvinyl chloride plastic waste using K/Na/Ca-modified iron ore oxygen carriers. Journal of Environmental Chemical Engineering. 2022, 10(2). https://doi.org/10.1016/j.jece.2022.107314.

[4]Marino A, Aloise A, Hernando H, et al. ZSM-5 zeolites performance assessment in catalytic pyrolysis of PVC-containing real WEEE plastic wastes. Catalysis Today. 2022, 390-391:210-20. https://doi.org/10.1016/j.cattod.2021.11.033.

[5]Plastics E, 2022. Plastics—The Facts (2021) An Analysis of European Latest Plastics Production, Demand and Waste Data. https://plasticseurope.org/knowledge-hub/plastics-the-facts-2021/ (20220530)

[6]Jiang G Z, Monsalve D A S, Clough P, et al. Understanding the Dechlorination of Chlorinated Hydrocarbons in the Pyrolysis of Mixed Plastics. ACS Sustainable Chemistry & Engineering. 2021, 9(4):1576-89. https://doi.org/10.1021/acssuschemeng.0c06461.

[7]Ling M, Ma D, Hu X, et al. Hydrothermal treatment of polyvinyl chloride: Reactors, dechlorination chemistry, application, and challenges. Chemosphere. 2023, 316:137718. https://doi.org/10.1016/j.chemosphere.2022.137718.

[8]Wang Y H, Wu K, Liu Q Y, et al. Low chlorine oil production through fast pyrolysis of mixed plastics combined with hydrothermal dechlorination pretreatment. Process Safety and Environmental Protection. 2021, 149:105-14. https://doi.org/10.1016/j.psep.2020.10.023.

[9]Xu Z, Kolapkar S, Zinchik S, et al. Comprehensive kinetic study of thermal degradation of polyvinylchloride (PVC). Polymer Degradation and Stability. 2020, 176. https://doi.org/ARTN 109148
10.1016/j.polymdegradstab.2020.109148.

[10]Ma D C, Liang L W, Hu E F, et al. Dechlorination of polyvinyl chloride by hydrothermal treatment with cupric ion. Process Safety and Environmental Protection. 2021, 146:108-17. https://doi.org/10.1016/j.psep.2020.08.040.

[11]Yang M L, Zhao P T, Cui X, et al. Kinetics study on hydrothermal dechlorination of poly(vinyl chloride) by in-situ sampling. Environmental Technology & Innovation. 2021, 23. https://doi.org/ARTN 101703
10.1016/j.eti.2021.101703.

[12]Yu Y, Zhu B X, Ding Y D, et al. Hydrothermal carbonization of food waste digestates and polyvinyl chloride: focus on dechlorination performance and fuel characteristics. Biomass Conversion And Biorefinery. 2022. https://doi.org/10.1007/s13399-022-02957-5.

[13]López A, de Marco I, Caballero B M, et al. Dechlorination of fuels in pyrolysis of PVC containing plastic wastes. Fuel Processing Technology. 2011, 92(2):253-60. https://doi.org/10.1016/j.fuproc.2010.05.008.

[14]Lopez-Urionabarrenechea A, de Marco I, Caballero B M, et al. Catalytic stepwise pyrolysis of packaging plastic waste. Journal of Analytical and Applied Pyrolysis. 2012, 96:54-62. https://doi.org/10.1016/j.jaap.2012.03.004.

[15]Dong N, Hui H, Li S, et al. Study on preparation of aromatic-rich oil by thermal dechlorination and fast pyrolysis of PVC. Journal of Analytical and Applied Pyrolysis. 2023, 169. https://doi.org/10.1016/j.jaap.2022.105817.

[16]Williams P. Yield and Composition of Gases and Oils-Waxes from the Feedstock Recycling of Waste Plastic. Chichester: John Wiley & Sons Ltd; 2006.

[17]Cao Q, Yuan G, Yin L, et al. Morphological characteristics of polyvinyl chloride (PVC) dechlorination during pyrolysis process: Influence of PVC content and heating rate. Waste Management. 2016, 58:241-9.

https://doi.org/10.1016/j.wasman.2016.08.031.
[18]Aggelopoulos C A, Svarnas P, Klapa M I, et al. Dielectric barrier discharge plasma used as a means for the remediation of soils contaminated by non-aqueous phase liquids. Chemical Engineering Journal. 2015, 270:428-36. https://doi.org/10.1016/j.cej.2015.02.056.
[19]Aggelopoulos C A. Atmospheric pressure dielectric barrier discharge for the remediation of soil contaminated by organic pollutants. International Journal Of Environmental Science And Technology. 2016, 13(7):1731-40. https://doi.org/10.1007/s13762-016-1009-0.
[20]Song J, Sima J, Pan Y, et al. Dielectric Barrier Discharge Plasma Synergistic Catalytic Pyrolysis of Waste Polyethylene into Aromatics-Enriched Oil. ACS Sustainable Chemistry & Engineering. 2021, 9(34):11448-57. https://doi.org/10.1021/acssuschemeng.1c03568.
[21]Song J, Wang J, Pan Y, et al. Catalytic pyrolysis of waste polyethylene into benzene, toluene, ethylbenzene and xylene (BTEX)-enriched oil with dielectric barrier discharge reactor. Journal of Environmental Management. 2022, 322. https://doi.org/10.1016/j.jenvman.2022.116096.
[22]Chung W-C, Chang M-B. Review of catalysis and plasma performance on dry reforming of CH4 and possible synergistic effects. Renewable Sustainable Energy Reviews. 2016, 62:13-31. https://doi.org/10.1016/j.rser.2016.04.007.
[23]Dębek R, Azzolina-Jury F, Travert A, et al. A review on plasma-catalytic methanation of carbon dioxide – Looking for an efficient catalyst. Renewable and Sustainable Energy Reviews. 2019, 116. https://doi.org/10.1016/j.rser.2019.109427.
[24]Xie W, Spectroscopic diagnostics of active species and their environmental chemical process of O2, N2, CO2 in cold plasma [D]. Academic Deprtment, Shanghai: Shanghai Jiao Tong University. 2008.
[25]Takaki K, Hatanaka Y, Arima K, et al. Influence of electrode configuration on ozone synthesis and microdischarge property in dielectric barrier discharge reactor. Vacuum. 2008, 83(1):128-32. https://doi.org/10.1016/j.vacuum.2008.03.047.
[26]Jodzis S, Zieba M. Energy efficiency of an ozone generation process in oxygen. Analysis of a pulsed DBD system. Vacuum. 2018, 155:29-37. https://doi.org/10.1016/j.vacuum.2018.05.035.
[27]Cui S P, Hao R L, Fu D. An integrated system of dielectric barrier discharge combined with wet electrostatic precipitator for simultaneous removal of NO and SO2: Key factors assessments, products analysis and mechanism. Fuel. 2018, 221:12-20. https://doi.org/10.1016/j.fuel.2018.02.078.
[28]Cai Y X, Zhu X B, Hu W S, et al. Plasma-catalytic decomposition of ethyl acetate over LaMO3 (M = Mn, Fe, and Co) perovskite catalysts. Journal Of Industrial And Engineering Chemistry. 2019, 70:447-52. https://doi.org/10.1016/j.jiec.2018.11.007.
[29]Liu S, Mei D, Nahil M, et al. Hybrid plasma-catalytic steam reforming of toluene as a biomass tar model compound over Ni/Al 2 O 3 catalysts. Fuel Processing Technology. 2017, 166:269-75. https://doi.org/10.1016/j.fuproc.2017.06.001.
[30]Liu S Y, Mei D H, Wang L, et al. Steam reforming of toluene as biomass tar model compound in a gliding arc discharge reactor. Chemical Engineering Journal. 2017, 307:793-802. https://doi.org/10.1016/j.cej.2016.08.005.
[31]Aminu I, Nahil M A, Williams P T. Hydrogen from Waste Plastics by Two-Stage Pyrolysis-Low-Temperature Plasma Catalytic Processing. Energy Fuels. 2020, 34:11679-89. https://doi.org/10.1021/acs.energyfuels.0c02043.
[32]Song J, Sun K, Huang Q. The effect of thermal aging on the composition of pyrolysis oil fuel derived from typical waste plastics. Fuel Processing Technology. 2021, 218. https://doi.org/10.1016/j.fuproc.2021.106862.
[33]Lofthus A, P. K. The spectrum of molecular nitrogen. Journal of Physical and Chemical Reference Data. 1977, 6(1).
[34]L. P, A. R. Emission spectroscopy study of N2-H2 glow discharge for metal surface nitriding. Journal of Physics D: Applied Physics. 1984, 17:919-29.
[35]Brüh S, M. R, G. G. A study by emission spectroscopy of the active species in pulsed DC discharges. Journal of Physics D: Applied Physics. 1997, 30:2917-22.

[36]Piper L G. State-to-state N2(A 3Σ+u) energy-pooling reactions. I. The formation of N2(C 3Πu) and the Herman infrared system. The Journal of Chemical Physics. 1988, 88(1):231-9. https://doi.org/10.1063/1.454649.
[37]Whitehead J C. Plasma–catalysis: the known knowns, the known unknowns and the unknown unknowns. Journal of Physics D: Applied Physics. 2016, 49(24). https://doi.org/10.1088/0022-3727/49/24/243001.
[38]Puliyalil H, Lašič Jurković D, Dasireddy V D B C, et al. A review of plasma-assisted catalytic conversion of gaseous carbon dioxide and methane into value-added platform chemicals and fuels. RSC Advances. 2018, 8(48):27481-508. https://doi.org/10.1039/c8ra03146k.
[39]Palma V, Cortese M, Renda S, et al. A Review about the Recent Advances in Selected NonThermal Plasma Assisted Solid-Gas Phase Chemical Processes. Nanomaterials (Basel). 2020, 10(8). https://doi.org/10.3390/nano10081596.
[40]Yoshioka T, Kameda T, Imai S, et al. Dechlorination of poly(vinyl chloride) using NaOH in ethylene glycol under atmospheric pressure. Polymer Degradation and Stability. 2008, 93(6):1138-41. https://doi.org/10.1016/j.polymdegradstab.2008.03.007.
[41]Pan J, Jiang H, Qing T, et al. Transformation and kinetics of chlorine-containing products during pyrolysis of plastic wastes. Chemosphere. 2021, 284:131348. https://doi.org/10.1016/j.chemosphere.2021.131348.
[42]Karayildirim T, Yanik J, Yuksel M, et al. The effect of some fillers on PVC degradation. Journal of Analytical and Applied Pyrolysis. 2006, 75(2):112-9. https://doi.org/10.1016/j.jaap.2005.04.012.
[43]Bhaskar T, Tanabe M, Muto A, et al. Analysis of chlorine distribution in the pyrolysis products of poly(vinylidene chloride) mixed with polyethylene, polypropylene or polystyrene. Polymer Degradation and Stability. 2005, 89(1):38-42. https://doi.org/10.1016/j.polymdegradstab.2004.12.022.
[44]Zhu H M, Jiang X G, Yan J H, et al. TG-FTIR analysis of PVC thermal degradation and HCl removal. Journal of Analytical and Applied Pyrolysis. 2008, 82(1):1-9. https://doi.org/10.1016/j.jaap.2007.11.011.
[45]Basan S, Guven O. A comparison of various isothermal thermogravimetric methods applied to the degradation of PVC. Thermochimica Acta. 1986, 106(15):169-78.
[46]Anthony G M. Kinetic and chemical studies of polymer cross-linking using thermal gravimetry and hyphenated methods. Degradation of polyvinylchloride. Polymer Degradation and Stability. 1999, 64(3):353-7.
[47]Bockhorn H, Hornung A, Hornung U. Mechanism and kinetics of thermal decomposition of plastics from isothermal and dynamic measurements. Journal of Analytical and Applied Pyrolysis. 1999, 50(2):77-101.
[48]Yuan G, Chen D, Yin L, et al. High efficiency chlorine removal from polyvinyl chloride (PVC) pyrolysis with a gas-liquid fluidized bed reactor. Waste Manag. 2014, 34(6):1045-50. https://doi.org/10.1016/j.wasman.2013.08.021.
[49]Knumann R, Bockhorn H. Investigation Of the Kinetics Of Pyrolysis Of Pvc by Tg-Ms-Analysis. Combustion Science And Technology. 1994, 101(1-6):285-99. https://doi.org/Doi 10.1080/00102209408951877.
[50]Marcilla A, Beltran M. Thermogravimetric Kinetic-Study Of Poly(Vinyl Chloride) Pyrolysis. Polymer Degradation and Stability. 1995, 48(2):219-29. https://doi.org/Doi 10.1016/0141-3910(95)00050-V.
[51]Wang Z, Xie T, Ning X Y, et al. Thermal degradation kinetics study of polyvinyl chloride (PVC) sheath for new and aged cables. Waste Management. 2019, 99:146-53. https://doi.org/10.1016/j.wasman.2019.08.042.